

Search for CP Violation in the Decay $\tau^- \rightarrow \pi^- K_s^0 (\geq 0\pi^0) \nu_\tau$

J. P. Lees,¹ V. Poireau,¹ V. Tisserand,¹ J. Garra Tico,² E. Grauges,² M. Martinelli^{ab,3} D. A. Milanes^{a,3},
A. Palano^{ab,3} M. Pappagallo^{ab,3} G. Eigen,⁴ B. Stugu,⁴ D. N. Brown,⁵ L. T. Kerth,⁵ Yu. G. Kolomensky,⁵
G. Lynch,⁵ H. Koch,⁶ T. Schroeder,⁶ D. J. Asgeirsson,⁷ C. Hearty,⁷ T. S. Mattison,⁷ J. A. McKenna,⁷ A. Khan,⁸
V. E. Blinov,⁹ A. R. Buzykaev,⁹ V. P. Druzhinin,⁹ V. B. Golubev,⁹ E. A. Kravchenko,⁹ A. P. Onuchin,⁹
S. I. Serednyakov,⁹ Yu. I. Skovpen,⁹ E. P. Solodov,⁹ K. Yu. Todyshev,⁹ A. N. Yushkov,⁹ M. Bondioli,¹⁰
D. Kirkby,¹⁰ A. J. Lankford,¹⁰ M. Mandelkern,¹⁰ D. P. Stoker,¹⁰ H. Atmacan,¹¹ J. W. Gary,¹¹ F. Liu,¹¹ O. Long,¹¹
G. M. Vitug,¹¹ C. Campagnari,¹² T. M. Hong,¹² D. Kovalskyi,¹² J. D. Richman,¹² C. A. West,¹² A. M. Eisner,¹³
J. Kroseberg,¹³ W. S. Lockman,¹³ A. J. Martinez,¹³ T. Schalk,¹³ B. A. Schumm,¹³ A. Seiden,¹³ C. H. Cheng,¹⁴
D. A. Doll,¹⁴ B. Echenard,¹⁴ K. T. Flood,¹⁴ D. G. Hitlin,¹⁴ P. Ongmongkolkul,¹⁴ F. C. Porter,¹⁴ A. Y. Rikitin,¹⁴
R. Andreassen,¹⁵ M. S. Dubrovin,¹⁵ Z. Huard,¹⁵ B. T. Meadows,¹⁵ M. D. Sokoloff,¹⁵ L. Sun,¹⁵ P. C. Bloom,¹⁶
W. T. Ford,¹⁶ A. Gaz,¹⁶ M. Nagel,¹⁶ U. Nauenberg,¹⁶ J. G. Smith,¹⁶ S. R. Wagner,¹⁶ R. Ayad,^{17,*} W. H. Toki,¹⁷
B. Spaan,¹⁸ M. J. Kobel,¹⁹ K. R. Schubert,¹⁹ R. Schwierz,¹⁹ D. Bernard,²⁰ M. Verderi,²⁰ P. J. Clark,²¹ S. Playfer,²¹
D. Bettoni^{a,22} C. Bozzi^{a,22} R. Calabrese^{ab,22} G. Cibinetto^{ab,22} E. Fioravanti^{ab,22} I. Garzia^{ab,22} E. Luppi^{ab,22}
M. Munerato^{ab,22} M. Negrini^{ab,22} L. Piemontese^{a,22} V. Santoro,²² R. Baldini-Ferrolì,²³ A. Calcaterra,²³
R. de Sangro,²³ G. Finocchiaro,²³ M. Nicolaci,²³ P. Patteri,²³ I. M. Peruzzi,^{23,†} M. Piccolo,²³ M. Rama,²³
A. Zallo,²³ R. Contri^{ab,24} E. Guido^{ab,24} M. Lo Vetere^{ab,24} M. R. Monge^{ab,24} S. Passaggio^{a,24} C. Patrignani^{ab,24}
E. Robutti^{a,24} B. Bhuyan,²⁵ V. Prasad,²⁵ C. L. Lee,²⁶ M. Morii,²⁶ A. J. Edwards,²⁷ A. Adametz,²⁸ J. Marks,²⁸
U. Uwer,²⁸ F. U. Bernlochner,²⁹ M. Ebert,²⁹ H. M. Lacker,²⁹ T. Lueck,²⁹ P. D. Dauncey,³⁰ M. Tibbetts,³⁰
P. K. Behera,³¹ U. Mallik,³¹ C. Chen,³² J. Cochran,³² W. T. Meyer,³² S. Prell,³² E. I. Rosenberg,³² A. E. Rubin,³²
A. V. Gritsan,³³ Z. J. Guo,³³ N. Arnaud,³⁴ M. Davier,³⁴ G. Grosdidier,³⁴ F. Le Diberder,³⁴ A. M. Lutz,³⁴
B. Malaescu,³⁴ P. Roudeau,³⁴ M. H. Schune,³⁴ A. Stocchi,³⁴ G. Wormser,³⁴ D. J. Lange,³⁵ D. M. Wright,³⁵
I. Bingham,³⁶ C. A. Chavez,³⁶ J. P. Coleman,³⁶ J. R. Fry,³⁶ E. Gabathuler,³⁶ D. E. Hutchcroft,³⁶ D. J. Payne,³⁶
C. Touramanis,³⁶ A. J. Bevan,³⁷ F. Di Lodovico,³⁷ R. Sacco,³⁷ M. Sigamani,³⁷ G. Cowan,³⁸ D. N. Brown,³⁹
C. L. Davis,³⁹ A. G. Denig,⁴⁰ M. Fritsch,⁴⁰ W. Gradl,⁴⁰ A. Hafner,⁴⁰ E. Prencipe,⁴⁰ K. E. Alwyn,⁴¹ D. Bailey,⁴¹
R. J. Barlow,^{41,‡} G. Jackson,⁴¹ G. D. Lafferty,⁴¹ E. Behn,⁴² R. Cenci,⁴² B. Hamilton,⁴² A. Jawahery,⁴²
D. A. Roberts,⁴² G. Simi,⁴² C. Dallapiccola,⁴³ R. Cowan,⁴⁴ D. Dujmic,⁴⁴ G. Sciolla,⁴⁴ D. Lindemann,⁴⁵
P. M. Patel,⁴⁵ S. H. Robertson,⁴⁵ M. Schram,⁴⁵ P. Biassoni^{ab,46} A. Lazzaro^{ab,46} V. Lombardo^{a,46} N. Neri^{ab,46}
F. Palombo^{ab,46} S. Stracka^{ab,46} L. Cremaldi,⁴⁷ R. Godang,^{47,§} R. Kroeger,⁴⁷ P. Sonnek,⁴⁷ D. J. Summers,⁴⁷
X. Nguyen,⁴⁸ P. Taras,⁴⁸ G. De Nardo^{ab,49} D. Monorchio^{ab,49} G. Onorato^{ab,49} C. Sciacca^{ab,49} G. Raven,⁵⁰
H. L. Snoek,⁵⁰ C. P. Jessop,⁵¹ K. J. Knoepfel,⁵¹ J. M. LoSecco,⁵¹ W. F. Wang,⁵¹ K. Honscheid,⁵² R. Kass,⁵²
J. Brau,⁵³ R. Frey,⁵³ N. B. Sinev,⁵³ D. Strom,⁵³ E. Torrence,⁵³ E. Feltresi^{ab,54} N. Gagliardi^{ab,54} M. Margoni^{ab,54}
M. Morandin^{a,54} M. Posocco^{a,54} M. Rotondo^{a,54} F. Simonetto^{ab,54} R. Stroili^{ab,54} S. Akar,⁵⁵ E. Ben-Haim,⁵⁵
M. Bomben,⁵⁵ G. R. Bonneaud,⁵⁵ H. Briand,⁵⁵ G. Calderini,⁵⁵ J. Chauveau,⁵⁵ O. Hamon,⁵⁵ Ph. Leruste,⁵⁵
G. Marchiori,⁵⁵ J. Ocariz,⁵⁵ S. Sitt,⁵⁵ M. Biasini^{ab,56} E. Manoni^{ab,56} S. Pacetti^{ab,56} A. Rossi^{ab,56} C. Angelini^{ab,57}
G. Batignani^{ab,57} S. Bettarini^{ab,57} M. Carpinelli^{ab,57,¶} G. Casarosa^{ab,57} A. Cervelli^{ab,57} F. Forti^{ab,57}
M. A. Giorgi^{ab,57} A. Lusiani^{ac,57} B. Oberhof^{ab,57} E. Paoloni^{ab,57} A. Perez^{a,57} G. Rizzo^{ab,57} J. J. Walsh^{a,57}
D. Lopes Pegna,⁵⁸ C. Lu,⁵⁸ J. Olsen,⁵⁸ A. J. S. Smith,⁵⁸ A. V. Telnov,⁵⁸ F. Anulli^{a,59} G. Cavoto^{a,59} R. Faccini^{ab,59}
F. Ferrarotto^{a,59} F. Ferroni^{ab,59} M. Gaspero^{ab,59} L. Li Gioi^{a,59} M. A. Mazzoni^{a,59} G. Piredda^{a,59} C. Büniger,⁶⁰
O. Grünberg,⁶⁰ T. Hartmann,⁶⁰ T. Leddig,⁶⁰ H. Schröder,⁶⁰ R. Waldi,⁶⁰ T. Adye,⁶¹ E. O. Olaiya,⁶¹ F. F. Wilson,⁶¹
S. Emery,⁶² G. Hamel de Monchenault,⁶² G. Vasseur,⁶² Ch. Yèche,⁶² D. Aston,⁶³ D. J. Bard,⁶³ R. Bartoldus,⁶³
C. Cartaro,⁶³ M. R. Convery,⁶³ J. Dorfan,⁶³ G. P. Dubois-Felsmann,⁶³ W. Dunwoodie,⁶³ R. C. Field,⁶³ M. Franco
Sevilla,⁶³ B. G. Fulsom,⁶³ A. M. Gabareen,⁶³ M. T. Graham,⁶³ P. Grenier,⁶³ C. Hast,⁶³ W. R. Innes,⁶³
M. H. Kelsey,⁶³ H. Kim,⁶³ P. Kim,⁶³ M. L. Kocian,⁶³ D. W. G. S. Leith,⁶³ P. Lewis,⁶³ S. Li,⁶³ B. Lindquist,⁶³
S. Luitz,⁶³ V. Luth,⁶³ H. L. Lynch,⁶³ D. B. MacFarlane,⁶³ D. R. Muller,⁶³ H. Neal,⁶³ S. Nelson,⁶³ I. Ofte,⁶³
M. Perl,⁶³ T. Pulliam,⁶³ B. N. Ratcliff,⁶³ A. Roodman,⁶³ A. A. Salnikov,⁶³ R. H. Schindler,⁶³ A. Snyder,⁶³ D. Su,⁶³

M. K. Sullivan,⁶³ J. Va'vra,⁶³ A. P. Wagner,⁶³ M. Weaver,⁶³ W. J. Wisniewski,⁶³ M. Wittgen,⁶³ D. H. Wright,⁶³
 H. W. Wulsin,⁶³ A. K. Yarritu,⁶³ C. C. Young,⁶³ V. Ziegler,⁶³ W. Park,⁶⁴ M. V. Purohit,⁶⁴ R. M. White,⁶⁴
 J. R. Wilson,⁶⁴ A. Randle-Conde,⁶⁵ S. J. Sekula,⁶⁵ M. Bellis,⁶⁶ J. F. Benitez,⁶⁶ P. R. Burchat,⁶⁶ T. S. Miyashita,⁶⁶
 M. S. Alam,⁶⁷ J. A. Ernst,⁶⁷ R. Gorodeisky,⁶⁸ N. Guttman,⁶⁸ D. R. Peimer,⁶⁸ A. Soffer,⁶⁸ P. Lund,⁶⁹
 S. M. Spanier,⁶⁹ R. Eckmann,⁷⁰ J. L. Ritchie,⁷⁰ A. M. Ruland,⁷⁰ C. J. Schilling,⁷⁰ R. F. Schwitters,⁷⁰ B. C. Wray,⁷⁰
 J. M. Izen,⁷¹ X. C. Lou,⁷¹ F. Bianchi^{ab},⁷² D. Gamba^{ab},⁷² L. Lanceri^{ab},⁷³ L. Vitale^{ab},⁷³ F. Martinez-Vidal,⁷⁴
 A. Oyanguren,⁷⁴ H. Ahmed,⁷⁵ J. Albert,⁷⁵ Sw. Banerjee,⁷⁵ H. H. F. Choi,⁷⁵ G. J. King,⁷⁵ R. Kowalewski,⁷⁵
 M. J. Lewczuk,⁷⁵ I. M. Nugent,⁷⁵ J. M. Roney,⁷⁵ R. J. Sobie,⁷⁵ N. Tasneem,⁷⁵ T. J. Gershon,⁷⁶ P. F. Harrison,⁷⁶
 T. E. Latham,⁷⁶ E. M. T. Puccio,⁷⁶ H. R. Band,⁷⁷ S. Dasu,⁷⁷ Y. Pan,⁷⁷ R. Prepost,⁷⁷ and S. L. Wu⁷⁷

(The BABAR Collaboration)

¹Laboratoire d'Annecy-le-Vieux de Physique des Particules (LAPP),
 Université de Savoie, CNRS/IN2P3, F-74941 Annecy-Le-Vieux, France

²Universitat de Barcelona, Facultat de Física, Departament ECM, E-08028 Barcelona, Spain

³INFN Sezione di Bari^a; Dipartimento di Fisica, Università di Bari^b, I-70126 Bari, Italy

⁴University of Bergen, Institute of Physics, N-5007 Bergen, Norway

⁵Lawrence Berkeley National Laboratory and University of California, Berkeley, California 94720, USA

⁶Ruhr Universität Bochum, Institut für Experimentalphysik 1, D-44780 Bochum, Germany

⁷University of British Columbia, Vancouver, British Columbia, Canada V6T 1Z1

⁸Brunel University, Uxbridge, Middlesex UB8 3PH, United Kingdom

⁹Budker Institute of Nuclear Physics, Novosibirsk 630090, Russia

¹⁰University of California at Irvine, Irvine, California 92697, USA

¹¹University of California at Riverside, Riverside, California 92521, USA

¹²University of California at Santa Barbara, Santa Barbara, California 93106, USA

¹³University of California at Santa Cruz, Institute for Particle Physics, Santa Cruz, California 95064, USA

¹⁴California Institute of Technology, Pasadena, California 91125, USA

¹⁵University of Cincinnati, Cincinnati, Ohio 45221, USA

¹⁶University of Colorado, Boulder, Colorado 80309, USA

¹⁷Colorado State University, Fort Collins, Colorado 80523, USA

¹⁸Technische Universität Dortmund, Fakultät Physik, D-44221 Dortmund, Germany

¹⁹Technische Universität Dresden, Institut für Kern- und Teilchenphysik, D-01062 Dresden, Germany

²⁰Laboratoire Leprince-Ringuet, Ecole Polytechnique, CNRS/IN2P3, F-91128 Palaiseau, France

²¹University of Edinburgh, Edinburgh EH9 3JZ, United Kingdom

²²INFN Sezione di Ferrara^a; Dipartimento di Fisica, Università di Ferrara^b, I-44100 Ferrara, Italy

²³INFN Laboratori Nazionali di Frascati, I-00044 Frascati, Italy

²⁴INFN Sezione di Genova^a; Dipartimento di Fisica, Università di Genova^b, I-16146 Genova, Italy

²⁵Indian Institute of Technology Guwahati, Guwahati, Assam, 781 039, India

²⁶Harvard University, Cambridge, Massachusetts 02138, USA

²⁷Harvey Mudd College, Claremont, California 91711

²⁸Universität Heidelberg, Physikalisches Institut, Philosophenweg 12, D-69120 Heidelberg, Germany

²⁹Humboldt-Universität zu Berlin, Institut für Physik, Newtonstr. 15, D-12489 Berlin, Germany

³⁰Imperial College London, London, SW7 2AZ, United Kingdom

³¹University of Iowa, Iowa City, Iowa 52242, USA

³²Iowa State University, Ames, Iowa 50011-3160, USA

³³Johns Hopkins University, Baltimore, Maryland 21218, USA

³⁴Laboratoire de l'Accélérateur Linéaire, IN2P3/CNRS et Université Paris-Sud 11,
 Centre Scientifique d'Orsay, B. P. 34, F-91898 Orsay Cedex, France

³⁵Lawrence Livermore National Laboratory, Livermore, California 94550, USA

³⁶University of Liverpool, Liverpool L69 7ZE, United Kingdom

³⁷Queen Mary, University of London, London, E1 4NS, United Kingdom

³⁸University of London, Royal Holloway and Bedford New College, Egham, Surrey TW20 0EX, United Kingdom

³⁹University of Louisville, Louisville, Kentucky 40292, USA

⁴⁰Johannes Gutenberg-Universität Mainz, Institut für Kernphysik, D-55099 Mainz, Germany

⁴¹University of Manchester, Manchester M13 9PL, United Kingdom

⁴²University of Maryland, College Park, Maryland 20742, USA

⁴³University of Massachusetts, Amherst, Massachusetts 01003, USA

⁴⁴Massachusetts Institute of Technology, Laboratory for Nuclear Science, Cambridge, Massachusetts 02139, USA

⁴⁵McGill University, Montréal, Québec, Canada H3A 2T8

⁴⁶INFN Sezione di Milano^a; Dipartimento di Fisica, Università di Milano^b, I-20133 Milano, Italy

⁴⁷University of Mississippi, University, Mississippi 38677, USA

⁴⁸Université de Montréal, Physique des Particules, Montréal, Québec, Canada H3C 3J7

- ⁴⁹INFN Sezione di Napoli^a; Dipartimento di Scienze Fisiche,
Università di Napoli Federico II^b, I-80126 Napoli, Italy
- ⁵⁰NIKHEF, National Institute for Nuclear Physics and High Energy Physics, NL-1009 DB Amsterdam, The Netherlands
- ⁵¹University of Notre Dame, Notre Dame, Indiana 46556, USA
- ⁵²Ohio State University, Columbus, Ohio 43210, USA
- ⁵³University of Oregon, Eugene, Oregon 97403, USA
- ⁵⁴INFN Sezione di Padova^a; Dipartimento di Fisica, Università di Padova^b, I-35131 Padova, Italy
- ⁵⁵Laboratoire de Physique Nucléaire et de Hautes Energies,
IN2P3/CNRS, Université Pierre et Marie Curie-Paris6,
Université Denis Diderot-Paris7, F-75252 Paris, France
- ⁵⁶INFN Sezione di Perugia^a; Dipartimento di Fisica, Università di Perugia^b, I-06100 Perugia, Italy
- ⁵⁷INFN Sezione di Pisa^a; Dipartimento di Fisica,
Università di Pisa^b; Scuola Normale Superiore di Pisa^c, I-56127 Pisa, Italy
- ⁵⁸Princeton University, Princeton, New Jersey 08544, USA
- ⁵⁹INFN Sezione di Roma^a; Dipartimento di Fisica,
Università di Roma La Sapienza^b, I-00185 Roma, Italy
- ⁶⁰Universität Rostock, D-18051 Rostock, Germany
- ⁶¹Rutherford Appleton Laboratory, Chilton, Didcot, Oxon, OX11 0QX, United Kingdom
- ⁶²CEA, Irfu, SPP, Centre de Saclay, F-91191 Gif-sur-Yvette, France
- ⁶³SLAC National Accelerator Laboratory, Stanford, California 94309 USA
- ⁶⁴University of South Carolina, Columbia, South Carolina 29208, USA
- ⁶⁵Southern Methodist University, Dallas, Texas 75275, USA
- ⁶⁶Stanford University, Stanford, California 94305-4060, USA
- ⁶⁷State University of New York, Albany, New York 12222, USA
- ⁶⁸Tel Aviv University, School of Physics and Astronomy, Tel Aviv, 69978, Israel
- ⁶⁹University of Tennessee, Knoxville, Tennessee 37996, USA
- ⁷⁰University of Texas at Austin, Austin, Texas 78712, USA
- ⁷¹University of Texas at Dallas, Richardson, Texas 75083, USA
- ⁷²INFN Sezione di Torino^a; Dipartimento di Fisica Sperimentale, Università di Torino^b, I-10125 Torino, Italy
- ⁷³INFN Sezione di Trieste^a; Dipartimento di Fisica, Università di Trieste^b, I-34127 Trieste, Italy
- ⁷⁴IFIC, Universitat de Valencia-CSIC, E-46071 Valencia, Spain
- ⁷⁵University of Victoria, Victoria, British Columbia, Canada V8W 3P6
- ⁷⁶Department of Physics, University of Warwick, Coventry CV4 7AL, United Kingdom
- ⁷⁷University of Wisconsin, Madison, Wisconsin 53706, USA
- (Dated: January 16, 2012)

Abstract

We report a search for CP violation in the decay $\tau^- \rightarrow \pi^- K_S^0 (\geq 0\pi^0) \nu_\tau$ using a dataset of 437 million τ lepton pairs, corresponding to an integrated luminosity of 476 fb^{-1} , collected with the BABAR detector at the PEP-II asymmetric energy e^+e^- storage rings. The CP -violating decay-rate asymmetry is determined to be $(-0.36 \pm 0.23 \pm 0.11)\%$ approximately 2.8 standard deviations from the Standard Model prediction of $(0.36 \pm 0.01)\%$.

PACS numbers: 13.35.Dx, 11.30.Er

CP violation has been observed only in the K and B meson systems. However, Bigi and Sanda [1] predict that, in the Standard Model (SM), the decay of the τ lepton to final states containing a K_S^0 meson will also have a non-zero decay-rate asymmetry due to CP violation in the kaon sector. The decay-rate asymmetry

$$A_Q = \frac{\Gamma(\tau^+ \rightarrow \pi^+ K_S^0 \bar{\nu}_\tau) - \Gamma(\tau^- \rightarrow \pi^- K_S^0 \nu_\tau)}{\Gamma(\tau^+ \rightarrow \pi^+ K_S^0 \bar{\nu}_\tau) + \Gamma(\tau^- \rightarrow \pi^- K_S^0 \nu_\tau)}$$

is predicted to be $(0.33 \pm 0.01)\%$ for decay times comparable to the lifetime $\tau_{K_S^0}$ of the K_S^0 meson. In a recent paper, Grossman and Nir [2] point out that Sanda and Bigi did not include the interference between the amplitudes of intermediate K_S^0 and K_L^0 which is as important as the

pure K_S^0 amplitude. Therefore the decay-rate asymmetry depends on the reconstruction efficiency as a function of the $K_S^0 \rightarrow \pi^+\pi^-$ decay time. If the selection is fully efficient for decay times that are long compared with the K_S^0 lifetime, then the predicted decay-rate asymmetry is almost unchanged relative to the prediction of Bigi and Sanda [1], due to a sign error [2].

If the measured decay-rate asymmetry shows a significant deviation from the SM value then this could be evidence for new physics. No evidence for CP violation has been found in related studies by BABAR and Belle in $D^+ \rightarrow K_S^0 \pi^+$ decays [3, 4], by the Belle collaboration in a study of the angular distribution of the decay products in $\tau^- \rightarrow \pi^- K_S^0 \nu_\tau$ decays [5], or by the CLEO collaboration [6].

This paper presents a measurement of A_Q using $\tau^- \rightarrow \pi^- K_S^0 (\geq 0\pi^0) \nu_\tau$ and charge conjugate decays. The SM asymmetry is identical for decays with any number of π^0 mesons. If there is an asymmetry due to new-physics dynamics, then the impact of including modes with one or more π^0 mesons may be different.

The analysis uses data recorded by the *BABAR* detector at the PEP-II asymmetric-energy e^+e^- collider, operated at center-of-mass (CM) energies of 10.58 GeV and 10.54 GeV at the SLAC National Accelerator Laboratory. The *BABAR* detector is described in detail in Ref. [7]. In particular, charged kaons and pions are differentiated by ionization (dE/dx) measurements in the silicon vertex detector and the drift chamber in combination with an internally reflecting Cherenkov detector, with identification efficiency greater than 90% for pions and kaons with momenta above 1.5 GeV/ c in the laboratory frame [8]. The probability of identifying a pion as a charged kaon is less than 2%. An electromagnetic calorimeter made of cesium iodide crystals provides energy measurements for electrons and photons, and an instrumented flux return detector identifies muons [9]. For momenta above 1 GeV/ c in the laboratory frame, electrons and muons are identified with efficiencies of approximately 92% and 70%, respectively. Based on an integrated luminosity of 476 fb $^{-1}$, the data sample contains approximately 875 million τ leptons.

Simulated event samples are used to estimate the purity of the data sample. The production of τ pairs is simulated with the KK2F Monte Carlo (MC) event generator [10]. Subsequent decays of the τ lepton, continuum $q\bar{q}$ events (where $q = u, d, s, c$), and final-state radiative effects are modeled with Tauola [11], JETSET [12], and PHOTOS [13], respectively. Passage of the particles through the detector is simulated by Geant4 [14].

The τ pair is produced back-to-back in the e^+e^- CM frame. As a result, the decay products of the two τ leptons can be separated from each other by dividing the event into two hemispheres – the “signal” hemisphere and the “tag” hemisphere – using the event thrust axis [15]. The event thrust axis is calculated using all charged particles and all photon candidates in the entire event. We select events with one prompt track and a $K_S^0 \rightarrow \pi^+ \pi^-$ candidate reconstructed in the signal hemisphere, and exactly one oppositely charged prompt track in the tag hemisphere. A prompt track is defined to be a track with its point of closest approach to the beam spot being less than 1.5 cm in the plane transverse to the e^- beam axis and less than 2.5 cm in the direction of the e^- beam axis. Furthermore, if a pair of tracks is consistent with coming from a K_S^0 or Λ decay, or from a γ conversion after a mass cut and a displaced vertex cut, neither track can be a prompt track. The components of momentum transverse to the e^- beam axis for each of these two prompt tracks must be greater than 0.1 GeV/ c in the laboratory frame. The event is rejected if the prompt

track in the signal hemisphere is identified to be coming from a charged kaon. A K_S^0 candidate is defined as a pair of oppositely charged pion candidates with invariant mass between 0.488 and 0.508 GeV/ c^2 ; furthermore, the distance between the beam spot and the $\pi^+ \pi^-$ vertex must be at least three times its uncertainty (the $\pi^+ \pi^-$ will be referred to as the “ K_S^0 candidate daughters”). To reduce backgrounds from non- τ -pair events, we require that the momentum of the charged particle in the tag hemisphere be less than 4 GeV/ c in the CM frame and be identified as an electron (e -tag) or a muon (μ -tag). To reduce backgrounds from Bhabha, $\mu^+\mu^-$, and $q\bar{q}$ events, we require the magnitude of the event thrust to be between 0.92 and 0.99.

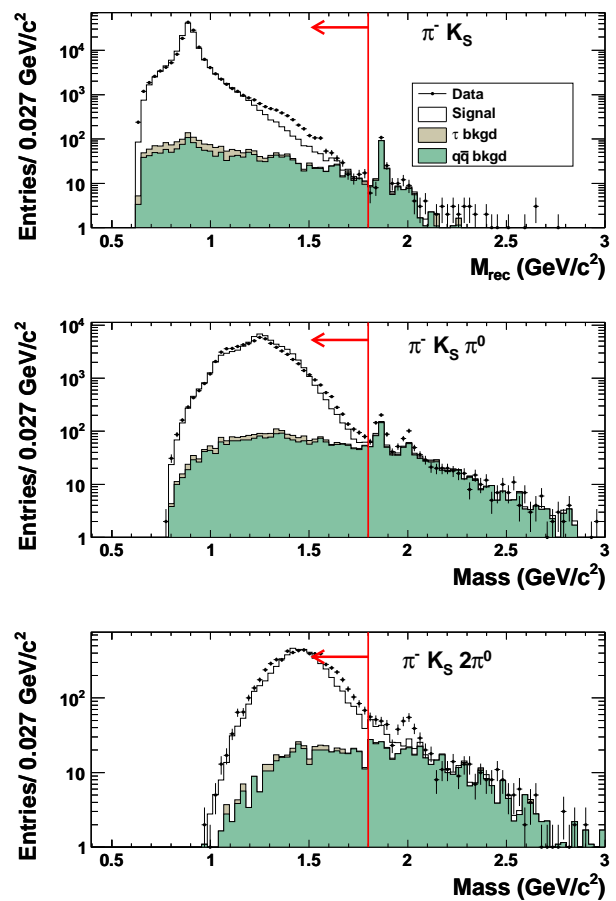
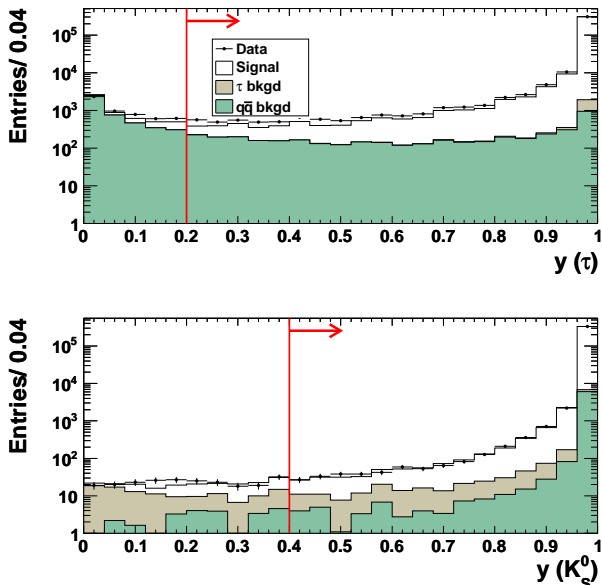


FIG. 1: Invariant-mass distributions for the combined e -tag and μ -tag samples. The label in each plot indicates the reconstructed decay mode (including the charge conjugate mode). Points with error bars represent data whereas the histograms represent the simulated sample. The histogram labeled as “Signal” includes the $\tau^- \rightarrow \pi^- K_S^0 (\geq 0\pi^0) \nu_\tau$, residual $\tau^- \rightarrow K^- K_S^0 (\geq 0\pi^0) \nu_\tau$, and $\tau^- \rightarrow \pi^- K^0 \bar{K}^0 \nu_\tau$ modes. All selection criteria (including the likelihood ratio requirement), except the invariant mass (M_{rec}) criterion, have been applied. The vertical lines and arrows indicate the $M_{\text{rec}} < 1.8$ GeV/ c^2 selection criterion.

97 Backgrounds from $q\bar{q}$ events are further reduced by re-123
 98 jecting events in which the invariant mass M_{rec} of the124
 99 charged particle (assumed to be a pion), the K_S^0 can-125
 100 didate, and up to three π^0 candidates, all in the signal126
 101 hemisphere, is greater than $1.8 \text{ GeV}/c^2$ (see Fig. 1). If127
 102 more than three π^0 candidates are reconstructed in the128
 103 signal hemisphere, the three with invariant masses clos-129
 104 est to the π^0 mass [16] are included in the calculation130
 105 of M_{rec} and the rest are ignored. The π^0 candidates131
 106 are constructed from two clusters of energy deposits in132
 107 the electromagnetic calorimeter that have no associated133
 108 tracks (“neutral clusters”). The energy of each cluster134
 109 is required to be greater than 30 MeV in the laboratory135
 110 frame, and the invariant mass of the two clusters must136
 111 be between $0.115 \text{ GeV}/c^2$ and $0.150 \text{ GeV}/c^2$. The number137
 112 of events in the $\tau^- \rightarrow \pi^- K_S^0 3\pi^0 \nu_\tau$ mode is small and138
 113 the corresponding invariant mass plot is not included in139
 114 Fig. 1. 140

115 The imperfect agreement between the M_{rec} distribu-141
 116 tions in the data and MC simulation, seen in Fig. 1, is142
 117 attributed to strange resonances that are not included143
 118 in the simulation. The impact of the modeling of the144
 119 τ decay modes in the MC simulation on the decay-rate145
 120 asymmetry is found to be small and is included in the146
 121 systematic uncertainties. 147



122 FIG. 2: The likelihood ratio $y(\tau)$ used to distinguish τ events169
 123 from $q\bar{q}$ events (top plot) and the likelihood ratio $y(K_S^0)$ used170
 124 to select τ decays with a $K_S^0 \rightarrow \pi^+\pi^-$ (bottom plot). All se-171
 125 lection cuts, except the plotted likelihood ratio requirement,172
 126 have been applied. Points with error bars represent data while173
 127 histograms correspond to simulated events. The histogram label-174
 128 ed as “Signal” includes the $\tau^- \rightarrow \pi^- K_S^0 (\geq 0\pi^0) \nu_\tau$, resid-175
 129 ual $\tau^- \rightarrow K^- K_S^0 (\geq 0\pi^0) \nu_\tau$, and $\tau^- \rightarrow \pi^- K^0 \bar{K}^0 \nu_\tau$ modes.176
 130 The vertical lines indicate the selection criteria. 177

131 events from $q\bar{q}$ events, and a second likelihood ratio
 132 $y(K_S^0)$ is used to reduce the background in the sam-
 133 ple of $K_S^0 \rightarrow \pi^+\pi^-$ candidates. The likelihood ratio
 134 $y_i(\vec{x}_i)$, where i refers to τ or K_S^0 , is defined as $y_i(\vec{x}_i) \equiv$
 135 $\mathcal{L}_i^s(\vec{x}_i)/(\mathcal{L}_i^s(\vec{x}_i) + w\mathcal{L}_i^b(\vec{x}_i))$ where w is the background-to-
 136 signal ratio estimated from the MC simulation, \mathcal{L}_i^s (\mathcal{L}_i^b)
 137 is the likelihood function for signal (background) events,
 138 and \vec{x}_i is the set of variables used for likelihood i . Each
 139 likelihood function is a product of one-dimensional prob-
 140 ability distribution functions of the variables \vec{x}_i obtained
 141 from the MC simulation. For $y(\tau)$, the variables \vec{x}_i are
 142 the visible energy (sum of the energies associated with
 143 all neutral calorimeter clusters and tracks in the event),
 144 the number of neutral clusters in the tag hemisphere, the
 145 number of neutral clusters in the signal hemisphere, the
 146 magnitude of the thrust, and the component of the total
 147 momentum of the event transverse to the e^- beam axis
 148 (calculated from all tracks and neutral clusters in both
 149 hemispheres). The variables used to construct $y(K_S^0)$ are
 150 the distance from the beam spot to the decay vertex of
 151 the K_S^0 candidate in the plane transverse to the e^- beam
 152 axis, the invariant mass of the K_S^0 candidate daughters,
 153 the magnitude of the K_S^0 momentum, and the cosine of
 154 the polar angle of the K_S^0 candidate. The polar angle is
 155 the angle between the K_S^0 trajectory and the e^- beam
 156 axis. The cosine of the polar angle discriminates low-
 157 angle photon conversions from genuine K_S^0 candidates.
 158 All kinematic quantities used in the construction of the
 159 two likelihood ratios, except for thrust, are determined
 160 in the laboratory frame. Events are selected if $y(\tau) > 0.2$
 161 and $y(K_S^0) > 0.4$ (see Fig. 2), in order to minimize the
 162 contamination from background events while maintain-
 163 ing a high selection efficiency. 164

165 After all selection criteria are applied, a total of 199064
 166 (140602) candidates are obtained in the e -tag (μ -tag)
 167 sample, of which there are 99842 (70369) in the τ^- sam-
 168 ple and 99222 (70233) in the τ^+ sample. 169

170 The sample contains events from two τ decay modes,
 171 $\tau^- \rightarrow K^- K_S^0 (\geq 0\pi^0) \nu_\tau$ and $\tau^- \rightarrow \pi^- K^0 \bar{K}^0 \nu_\tau$, that also
 172 have K_S^0 mesons in the final state. The decay $\tau^- \rightarrow$
 173 $\pi^- K^0 \bar{K}^0 \nu_\tau$ satisfies the selection criteria if one of the
 174 neutral kaons decays into $\pi^+\pi^-$ and the other neutral
 175 kaon decays into $2\pi^0$ or appears as a K_L^0 meson. 176

177 The selected candidate sample also contains a small
 178 background component from τ decays not containing a
 179 K_S^0 in the final state, as well as continuum $q\bar{q}$ (u , d , s
 180 and c -quark) events. There is no background from $B\bar{B}$
 181 events. 182

183 The numbers of background events of each type are
 184 estimated from the MC simulation. The accuracy of
 185 the background estimation is evaluated by measuring
 186 the ratios of data to simulated event yields in the re-
 187 gion $y(\tau) < 0.1$ and $y(K_S^0) < 0.1$. A correction factor is
 188 then applied to the background yield estimated from the
 189 Monte Carlo simulation in this region. The correction
 190 factors are determined to be 0.81 ± 0.03 (0.49 ± 0.03) for
 191 τ^- (τ^+) events. 192

the $q\bar{q}$ background and 0.9 ± 0.4 (1.0 ± 0.4) for the non- K_S^0 τ background in the e -tag (μ -tag) samples, respectively. The total numbers of background events are then estimated to be 1393 ± 79 (1120 ± 65) for τ^- decays and 1401 ± 74 (1055 ± 74) for τ^+ decays in the e -tag (μ -tag) samples, where all selection criteria (including the requirements on the two likelihood ratios) are applied. The uncertainties include the statistical uncertainties from the sizes of the Monte Carlo samples and the uncertainties of the correction factors. The composition of the sample is given Table I.

After the subtraction of background composed of $q\bar{q}$ and non- K_S^0 τ decays, the decay-rate asymmetry is measured to be $(-0.32 \pm 0.23)\%$ for the e -tag sample and $(-0.05 \pm 0.27)\%$ for the μ -tag sample, where the errors are statistical.

TABLE I: Breakdown of the sample after all selection criteria have been applied. The errors of the decay modes with K_S^0 are dominated by the uncertainties in the branching fractions. The background from other τ decays and $e^+e^- \rightarrow q\bar{q}$ background are estimated using the data and MC simulation samples.

Source	Fractions (%)	
	e -tag	μ -tag
$\tau^- \rightarrow \pi^- K_S^0(\geq 0\pi^0) \nu_\tau$	78.7 ± 4.0	78.4 ± 4.0
$\tau^- \rightarrow K^- K_S^0(\geq 0\pi^0) \nu_\tau$	4.2 ± 0.3	4.1 ± 0.3
$\tau^- \rightarrow \pi^- K^0 \bar{K}^0 \nu_\tau$	15.7 ± 3.7	15.9 ± 3.7
Other background	1.40 ± 0.06	1.55 ± 0.07

A control sample of $\tau^- \rightarrow h^- h^- h^+(\geq 0\pi^0) \nu_\tau$ (excluding $K_S^0 \rightarrow \pi^+\pi^-$ decays) in both data and MC simulation, where h^- (h^+) represents a negatively (positively) charged hadron, is used to confirm that no significant decay-rate asymmetry is induced by the *BABAR* detector or the selection criteria. The control sample is selected by requiring that all charged tracks be prompt tracks, which suppresses K_S^0 contamination due to its displaced decay vertex. The asymmetries measured in the simulated and data control samples agree to within the experimental uncertainties of the measurements, which are 0.12% for the e -tag and 0.08% for the μ -tag, and include both statistical and systematic components. These errors are taken as systematic uncertainties on the signal asymmetry (see Table II).

Additional studies show no evidence for any charge-dependent biases in the selection criteria. We find no decay-rate asymmetry in the MC sample of $\tau^- \rightarrow \pi^- K_S^0(\geq 0\pi^0) \nu_\tau$ decays (no CP violation is modeled in the simulation) where the error on the decay-rate asymmetries is 0.14% for the e -tag and 0.17% for the μ -tag events. We vary the selection criteria around their nominal values, and no significant changes in the asymmetry

TABLE II: Summary of systematic uncertainties in the decay-rate asymmetries.

	e -tag	μ -tag
Detector and selection bias	0.12%	0.08%
Background subtraction	0.05%	0.06%
K^0/\bar{K}^0 interaction	0.01%	0.01%
Total	0.13%	0.10%

are observed. The decay-rate asymmetry of the background events was studied by examining the events rejected by the likelihood ratio criteria and was found to be consistent with zero for both data and MC simulation.

A recent paper [17] suggests that the decay-rate asymmetry will be modified due to the different nuclear-interaction cross sections of the K^0 and \bar{K}^0 mesons with the material in the detector. This effect is not included in the MC simulation. A correction to the asymmetry accounting for this effect is calculated on an event-by-event basis using the momentum and polar angle of the K_S^0 candidate together with the nuclear-interaction cross sections for neutral kaons, which are related by isospin symmetry to the K^\pm nucleon cross sections [16]. The kaon-nucleon cross sections are determined by using the kaon-nucleon cross sections and including a nuclear screening factor of $A^{0.76}$, where A is the atomic weight [17]. The correction, which is subtracted from the measured asymmetry, is found to be $(0.07 \pm 0.01)\%$ for both the e -tag and the μ -tag samples. The error includes the statistical uncertainty in the MC simulation, the uncertainties in the kaon-nucleon cross sections [16], and an uncertainty due to the assumption of isospin invariance. The latter effect is taken to be 5% by observing that isospin symmetry in pion-nucleon cross sections holds to within a few percent. The error on the exponent of the atomic weight of the nuclear screening factor is 0.003 [17] and its contribution to the uncertainty in the asymmetry correction is negligible.

The measured decay-rate asymmetries (after correcting for the difference in neutral kaon nuclear interactions) are $(-0.39 \pm 0.23 \pm 0.13)\%$ for the e -tag sample and $(-0.12 \pm 0.27 \pm 0.10)\%$ for the μ -tag sample, where the first error is statistical and the second is systematic. The systematic uncertainties of the e -tag and μ -tag results are almost completely uncorrelated. The small correlations in the systematic uncertainties for the two samples are ignored when the average is computed. The weighted average of the two decay-rate asymmetries is $(-0.27 \pm 0.18 \pm 0.08)\%$.

The asymmetry measured at this stage still includes other τ decays with K_S^0 in the final state. Specifically, the decay-rate asymmetry is diluted due to $\tau^- \rightarrow K^- K_S^0 \nu_\tau$ and $\tau^- \rightarrow \pi^- K^0 \bar{K}^0 \nu_\tau$ decays. The measured asymmetry \mathcal{A} is related to the signal asymmetry \mathcal{A}_1 and the remain-

ing background asymmetries A_2 and A_3 by:

$$\begin{aligned} \mathcal{A} &= \frac{f_1 A_1 + f_2 A_2 + f_3 A_3}{f_1 + f_2 + f_3} \\ &= \left(\frac{f_1 - f_2}{f_1 + f_2 + f_3} \right) A_Q \end{aligned}$$

where f_1 , f_2 , and f_3 are, respectively, the fractions of $\tau^- \rightarrow \pi^- K_S^0 (\geq 0\pi^0) \nu_\tau$, $\tau^- \rightarrow K^- K_S^0 (\geq 0\pi^0) \nu_\tau$, and $\tau^- \rightarrow \pi^- K^0 \bar{K}^0 \nu_\tau$ in the total selected sample, shown in Table I. Within the SM, $A_1 = -A_2$ because the K_S^0 in $\tau^- \rightarrow \pi^- K_S^0 (\geq 0\pi^0) \nu_\tau$ is produced via a \bar{K}^0 , whereas the K_S^0 in $\tau^- \rightarrow K^- K_S^0 (\geq 0\pi^0) \nu_\tau$ is produced via a K^0 . Furthermore, $A_3 = 0$ in the SM because the asymmetries due to the K^0 and \bar{K}^0 will cancel each other. Using the relations between A_1 , A_2 , and A_3 , we can compare our result with the theoretical prediction by dividing the measured decay-rate asymmetry of $\mathcal{A} = (-0.27 \pm 0.18 \pm 0.08)\%$ by $(f_1 - f_2)/(f_1 + f_2 + f_3) = 0.75 \pm 0.04$ (the correction is identical for the e -tag and μ -tag samples). The uncertainty on the correction includes the statistical uncertainty and uncertainties in the branching fractions. Finally, the decay-rate asymmetry for the $\tau^- \rightarrow \pi^- K_S^0 (\geq 0\pi^0) \nu_\tau$ decay for the combined e -tag and μ -tag sample is calculated to be $A_Q = (-0.36 \pm 0.23 \pm 0.11)\%$.

As pointed out by Grossman and Nir, the predicted decay-rate asymmetry is affected by the $K_S^0 \rightarrow \pi^+ \pi^-$ decay time dependence of the event selection efficiency [2]. Figure 3 shows the relative selection efficiency, defined as the selection efficiency normalized to unity in the range $0.25 < t/\tau_{K_S^0} < 1.0$. In the $0 < t/\tau_{K_S^0} < 1$ region, the relative efficiency is parametrized with the function $(1 - Ae^{-B(t-t_0)})^{-2}$, where A , B , and t_0 are constants. In the $1 < t/\tau_{K_S^0} < 8$ region, the relative efficiency is parametrized by a second-order polynomial. Both functions are constrained to unity at $t/\tau_{K_S^0} = 1$. We use this parametrization in Eq. (13) of the Grossman and Nir paper [2] to obtain a multiplicative correction factor of 1.08 ± 0.01 for the decay-rate asymmetry, where the error is due to the uncertainty in the relative selection efficiency. After applying the correction factor, the SM decay-rate asymmetry is predicted to be $(0.36 \pm 0.01)\%$.

In conclusion, we have performed a search for CP violation using the $\tau^- \rightarrow \pi^- K_S^0 (\geq 0\pi^0) \nu_\tau$ decay mode. The decay-rate asymmetry is measured for the first time and is found to be $(-0.36 \pm 0.23 \pm 0.11)\%$. The measurement is 2.8 standard deviations from the SM prediction of $(0.36 \pm 0.01)\%$.

The authors thank Y. Grossman and Y. Nir for their useful suggestions. We are grateful for the excellent luminosity and machine conditions provided by our PEP-II colleagues, and for the substantial dedicated effort from the computing organizations that support BABAR. The collaborating institutions wish to thank SLAC for its support and kind hospitality. This work is supported by DOE and NSF (USA), NSERC (Canada), CEA and

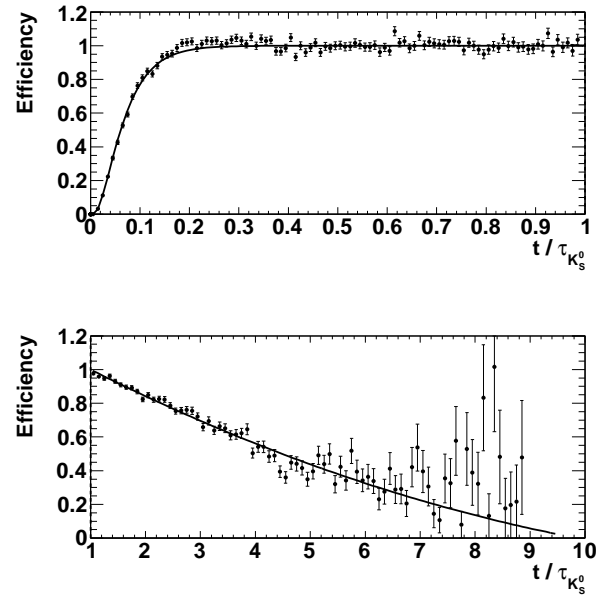


FIG. 3: The relative selection efficiency as a function of $t/\tau_{K_S^0}$ obtained from the Monte Carlo sample. The top plot shows the region $0 < t/\tau_{K_S^0} < 1$ and the bottom plot the region $1 < t/\tau_{K_S^0} < 8$. The solid line is the fit to the points in the displayed region. The relative efficiency is normalized to be unity for the region $0.25 < t/\tau_{K_S^0} < 1.0$.

CNRS-IN2P3 (France), BMBF and DFG (Germany), INFN (Italy), FOM (The Netherlands), NFR (Norway), MES (Russia), MICIIN (Spain), STFC (United Kingdom). Individuals have received support from the Marie Curie EIF (European Union), the A. P. Sloan Foundation (USA) and the Binational Science Foundation (USA-Israel).

* Now at Temple University, Philadelphia, Pennsylvania 19122, USA

† Also with Università di Perugia, Dipartimento di Fisica, Perugia, Italy

‡ Now at the University of Huddersfield, Huddersfield HD1 3DH, UK

§ Now at University of South Alabama, Mobile, Alabama 36688, USA

¶ Also with Università di Sassari, Sassari, Italy

- [1] I. I. Bigi and A. I. Sanda, Phys. Lett. B **625**, 47 (2005).
- [2] Y. Grossman and Y. Nir, arXiv:1110.3790 [hep-ph] (2011).
- [3] P. del Amo Sanchez *et al.* (BABAR Collaboration), Phys. Rev. D **83**, 071103 (2011).
- [4] B. R. Ko *et al.* (Belle Collaboration), Phys. Rev. Lett. **104**, 181602 (2010).
- [5] M. Bischofberger *et al.* (Belle Collaboration), Phys. Rev.

- 337 Lett. **107**, 131801 (2011). 349
- 338 [6] G. Bonvicini *et al.* (CLEO Collaboration), Phys. Rev. 350
339 Lett. **88**, 111803 (2002). 351
- 340 [7] B. Aubert *et al.* (BABAR Collaboration), Nucl. Instr. 352
341 Methods Phys. Res., Sect. A **479**, 1 (2002). 353
- 342 [8] B. Aubert *et al.* (BABAR Collaboration), Phys. Rev. Lett. 354
343 **99**, 021603 (2007). 355
- 344 [9] J. P. Lees *et al.* (BABAR Collaboration), Phys. Rev. D **81**, 356
345 111101(R) (2010). 357
- 346 [10] B. F. L. Ward, S. Jadach, and Z. Was, Nucl. Phys. Proc. 358
347 Suppl. **116**, 73 (2003). 359
- 348 [11] S. Jadach *et al.*, Comput. Phys. Commun. **76**, 361 (1993).
- [12] T. Sjostrand, Comput. Phys. Commun. **82**, 74 (1994).
- [13] E. Barberio and Z. Was, Comput. Phys. Commun. **79**,
291 (1994).
- [14] S. Agostinelli *et al.*, (Geant4 Collaboration) Nucl. Instr.
Methods Phys. Res., Sect. A **506**, 250 (2003).
- [15] S. Brandt *et al.*, Phys. Lett. **12**, 57 (1964); E. Farhi,
Phys. Rev. Lett. **39**, 1587 (1977).
- [16] K. Nakamura *et al.* (Particle Data Group), J. Phys. **G**
37, 075021 (2010) and 2011 partial update for the 2012
edition.
- [17] B. R. Ko *et al.*, arXiv:1006.1938 [hep-ex] (2010).